

Synthesis and evaluation of catecholase activities of metal complexes of 1,4-substituted piperazine Mannich base of 4-acetamidophenol

Ayowole Olaolu AYENI^{1,2,*}, Gareth Mostyn WATKINS¹¹Department of Chemistry, Rhodes University, Grahamstown, South Africa²Department of Chemistry, Obafemi Awolowo University, Ile Ife, Nigeria

Received: 09.10.2017

Accepted/Published Online: 29.01.2018

Final Version: 29.01.2018

Abstract: The synthesis and characterisation including ¹H and ¹³C NMR spectroscopy of a Mannich base 1,4-di-(5-acetamido-2-hydroxybenzyl)piperazine is herein reported. The Mannich reaction leading to the formation of the ligand took place at both ends of piperazine. Four metal complexes [Cu(II) and Fe(III)] including those bearing thiocyanate groups (SCN⁻) in N- and S-bonding modes have been studied for their abilities to mimic catecholase oxidase. All the metal complexes are catalytically active with the highest turnover rate (*k_{cat}*) recorded for complex **3**. The catalytic process as monitored by ¹H NMR spectroscopy (isolation of 3, 5-DTBQ) and iodometric titration revealed the formation of H₂O₂ and thus implied that the mechanism of oxidation is through the formation of a semiquinolate species.

Key words: Mannich base, thiocyanate, isothiocyanate, catecholase activity, turnover rates

1. Introduction

Oxidation processes are of wide relevance to the survival of plant and animal species and many of the processes require the activation of molecular oxygen. Coordination compounds are receiving greater attention owing to their abilities to biomimic the activities of some of the enzymes encountered in nature's oxidation processes.¹⁻⁴ An example of such oxidation processes is that of catechol, which is performed in nature by catecholase oxidase and is very important in higher plants to form quinones. Quinones are known to auto-polymerize to give melanin, thereby protecting plant tissues from damage by pathogens and insects.⁵ Also important are catechol dioxygenases that contain Fe(III) centres, e.g., catechol dioxygenases are important in the cleavage of catechol.^{6,7} Geometrical consideration around metal centres is vital in designing both mono- and dinuclear metal complexes with better biomimetic capabilities.⁸ Though several mechanistic pathways have been proposed, a lot of coordination compounds that biomimic catecholase oxidase are known to do so through an alternate pathway that involves the production of quinone along with H₂O₂ rather than water.⁹

Anbu and Kandaswamy have previously reported the DNA binding and catecholase activity of mono- and di-copper(II) complexes of 6,6'-piperazine-1,4-diyl-dimethylene-bis(4-methyl phenol), a 1,4-disubstituted Mannich base of p-cresol similar to the one reported herein.¹⁰ Metal complexes of Mannich bases possess great chelating effect properties and are worthy candidates for catecholase activity. Those from piperazine with Mannich reaction occurring at both ends though not widely encountered should be investigated for their biomimetic abilities with detailed kinetic studies carried out. The report herein is focused on the catecholase activity with

*Correspondence: aayeni@oauife.edu.ng

detailed kinetic studies of Cu(II) and Fe(III) complexes of a new Mannich base of 4-acetamidophenol. The influence of thiocyanate groups on the catecholase activity of the metal complexes is clearly outlined.

2. Results and discussion

The ligand was prepared and recrystallized from a chloroform:ethanol mixture with the spectroscopic characterisation reported for the first time to the best of our knowledge. The molecular structure was confirmed by ^1H and ^{13}C NMR spectroscopy alongside other techniques. The Cu(II) and Fe(III) complexes were also prepared and their structures were confirmed by various analytical and spectroscopic techniques. The molar conductance values of the complexes (measured in 10^{-3} M DMSO solution) show that only two of the metal complexes are electrolytic in nature; copper(II) complex **2** is a 1:1 electrolyte while iron(III) complex **4** is a 1:2 electrolyte.¹¹ Solubility of metal complexes is low in water, ethanol, chloroform, and most organic solvents, but high in DMSO and DMF and all the compounds have high melting points.

2.1. Nuclear magnetic resonance spectroscopy

The ligand was examined by ^1H and ^{13}C NMR spectroscopy. The formation of the ligand is strongly supported by the observation of the amino methyl ($\text{Ar}-\text{CH}_2-\text{N}-$) signal at 3.79 and 58.3 ppm in the ligand for proton and carbon spectra, respectively.^{12,13} Moreover, the signal of the methyl group of the acetamido substituent at the para-position to the hydroxyl in the ligand appears upfield as a singlet. In addition, the protons and the carbons within the piperazine are isoelectronic as all the signals appear upfield (at 2.90 and 52.0 ppm for proton and carbon signals, respectively), indicating the involvement of both (NH) groups of the piperazine in the Mannich reaction.

2.2. IR spectral analysis

According to elemental analysis, only in **1** is the metal ion coordinated to the deprotonated ligand, while **3** is the only mononuclear complex within this group. The stretching frequency of the phenolic OH was observed at 3250 cm^{-1} as a medium intense band suggesting minimal H-bonding. Positive shifts of $\sim 3\text{--}49\text{ cm}^{-1}$ are observed in the spectra of the metal complexes compared to that of the ligand. The bands observed at $3253\text{--}3299\text{ cm}^{-1}$ in the spectra of the metal complexes are broad and suggest the presence of coordinated water molecules may overlap the bonded hydroxyl group.¹⁴ Decrease in the stretching frequency is expected upon complexation and that is true for all the complexes as observed by the reduction in the $\nu\text{C}-\text{O}$ from 1297 cm^{-1} to about 1260 cm^{-1} in the metal complexes.¹⁵

The coordination of the N atom of the amine component of the Mannich base with the central metal ion is supported by the lowering of the stretching frequency of the νCNC of the ligand at 1141 cm^{-1} by $\sim 22\text{--}71\text{ cm}^{-1}$ upon complexation with the greatest reduction observed in **2**. The bands also became broader upon complexation and this lends further support to coordination of the group with metal ions.¹⁶

Thiocyanate and isothiocyanate bonding modes are predicted due to the observation of the stretching vibration (νCN) at 2106 cm^{-1} for **2** and 2035 cm^{-1} for **4**. These assignments are closely supported by the observation of the νCS in the range $739\text{--}798\text{ cm}^{-1}$.¹⁷

2.3. Electronic spectra of the ligand and its complexes

Maximum absorbance (λ_{max}) observed in the ligand at 33,670 and 33,445 cm^{-1} in DMF and DMSO, respectively, and is attributed to $\pi - \pi^*$ intraligand transition. The band observed for complex **1** at 21,459 cm^{-1} is thought to be a charge transfer band that appears to obscure the d-d transition in DMF. Two transitions, however, are observed in DMSO, the charge transfer band at 20921 cm^{-1} , while it appears that complex **1** assumed a square planar geometry in DMSO evidenced by the band observed at 11,682 cm^{-1} . Complex **2** showed similar but lower energies in DMSO compared to DMF in the range 16,103–14,970 cm^{-1} with the square planar geometry proposed. Ligand to metal charge transfer transition is expected for complex **2** and is only recorded at 22,779 cm^{-1} in DMSO.¹⁸

As previously reported, the electronic spectra of the Fe(III) complexes are dominated by $\pi - \pi^*$ and $n - \pi^*$ transitions of the ligand with octahedral geometry generally encountered.¹⁹ All the iron(III) complexes display a medium to intense band in the range 28,902–18,797 cm^{-1} in DMF and 28,571–19,841 cm^{-1} in DMSO. This transition each in **3** and **4** is assigned to the charge transfer transition and/or d-d transition peculiar to an Fe^{3+} ion in an 7-coordinate and octahedral configuration, respectively. The proposed structures are given in Figure 1 below.

2.4. Catechol oxidation activity

The catalytic activities of the complexes **1–4** towards the most common substrate 3,5-di-tert-butylcatechol (3,5-DTBC) in DMF solution under aerobic condition were studied. Wavelength scans revealed a gradual appearance of a new band with increasing intensity at ~ 399 nm (Figure 2).

The kinetics of oxidation of 3,5-DTBC by **1–4** were determined by the method of initial rates with the results presented in Figure 3 and that involved monitoring the growth of the quinone band at 399 nm as a function of time.^{20,21}

The rate constant versus concentration of the substrate data were then analysed on the basis of the Michaelis–Menten approach of enzyme kinetics (Figure 4) to get the Lineweaver–Burk plot (double reciprocal) presented in Figure 5, as well as the values of the Michaelis binding constant (K_M), maximum velocity (V_{max}), and rate constant for the dissociation of the substrate (i.e. turnover rates k_{cat}).

The kinetics data are listed in the Table; high k_{cat} values correspond to high catalytic efficiency. The catalytic efficiency is in the order **3** > **1** > **2** > **4**. In complex **3**, a 7-coordinate geometry is the most catalytically active, while **4** is the least catalytically active. In general, the presence of thiocyanate negatively impacts catecholase activity as previously observed in similar biomimetic studies.^{22,23}

Table. Kinetic parameters for the oxidation of 3,5-DTBC to 3,5-DTBQ mediated by **1–4** in DMF.

Complex	V_{max} (M min^{-1})	K_M (M)	k_{cat} (h^{-1})
1	$(2.65 \pm 0.12) \times 10^{-7}$	$(1.50 \pm 0.06) \times 10^{-3}$	9.54 ± 0.54
2	$(1.45 \pm 0.08) \times 10^{-7}$	$(6.77 \pm 0.35) \times 10^{-4}$	5.22 ± 0.22
3	$(3.36 \pm 0.14) \times 10^{-7}$	$(1.97 \pm 0.04) \times 10^{-3}$	12.96 ± 0.71
4	$(1.42 \pm 0.08) \times 10^{-7}$	$(2.38 \pm 0.12) \times 10^{-4}$	5.12 ± 0.22

The values of the turnover rates as presented in the Table are quite comparable to previously reported values in the literature.^{24,25}

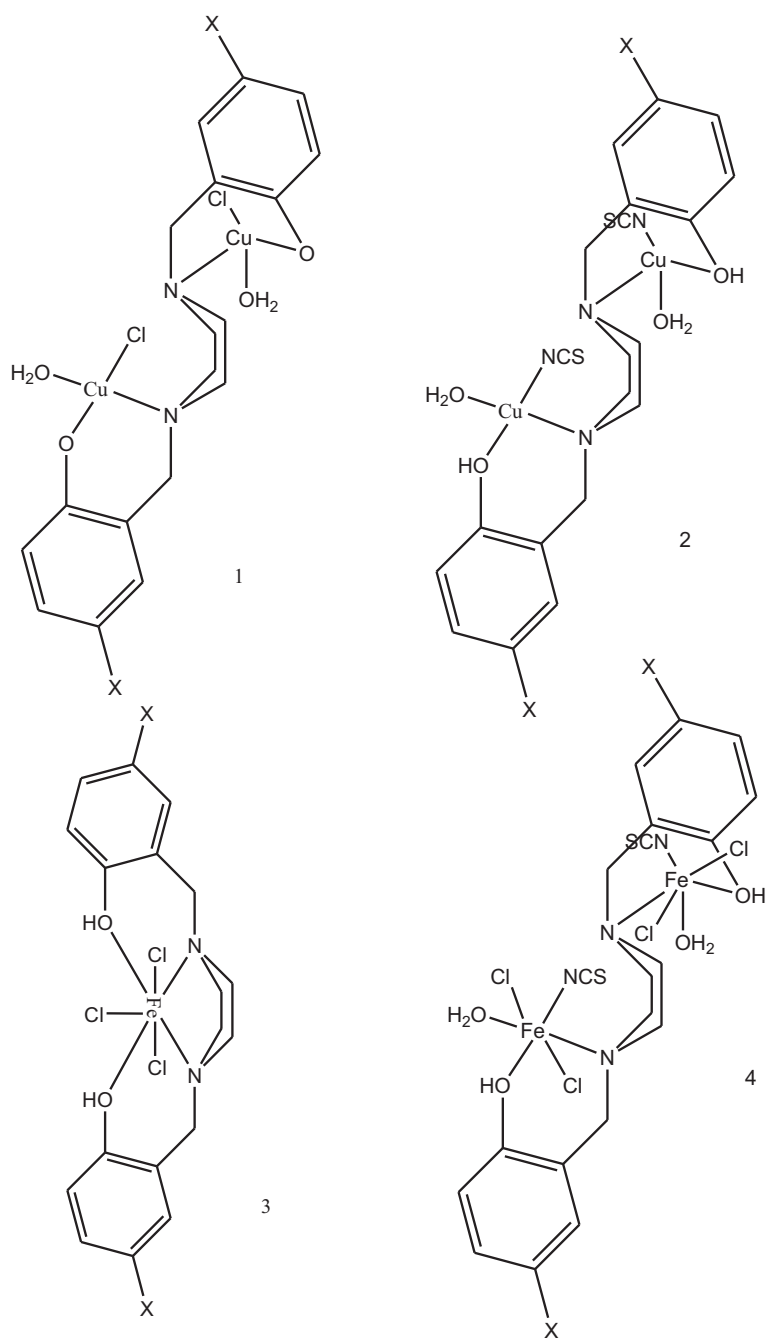


Figure 1. Proposed structures of metal complexes 1–4.

2.5. Probable mechanism of catecholase activity of the complexes

The identification of 3,5-DTBQ by ¹H NMR spectroscopy [¹H NMR (CDCl₃, 300 MHz): δ_H = 1.22 (s, 9H), 1.27 (s, 9H), 6.22 (d, *J* = 3.0 Hz, 1H), 6.92 (d, *J* = 3.0 Hz, 1H)] and H₂O₂ through iodometric titration points to the fact that the mechanism is as follows: one-electron transfer from catechol to the Cu(II) centre results in the formation of semiquinone radical and the Cu(II) centre is reduced to Cu(I). Dioxygen then binds

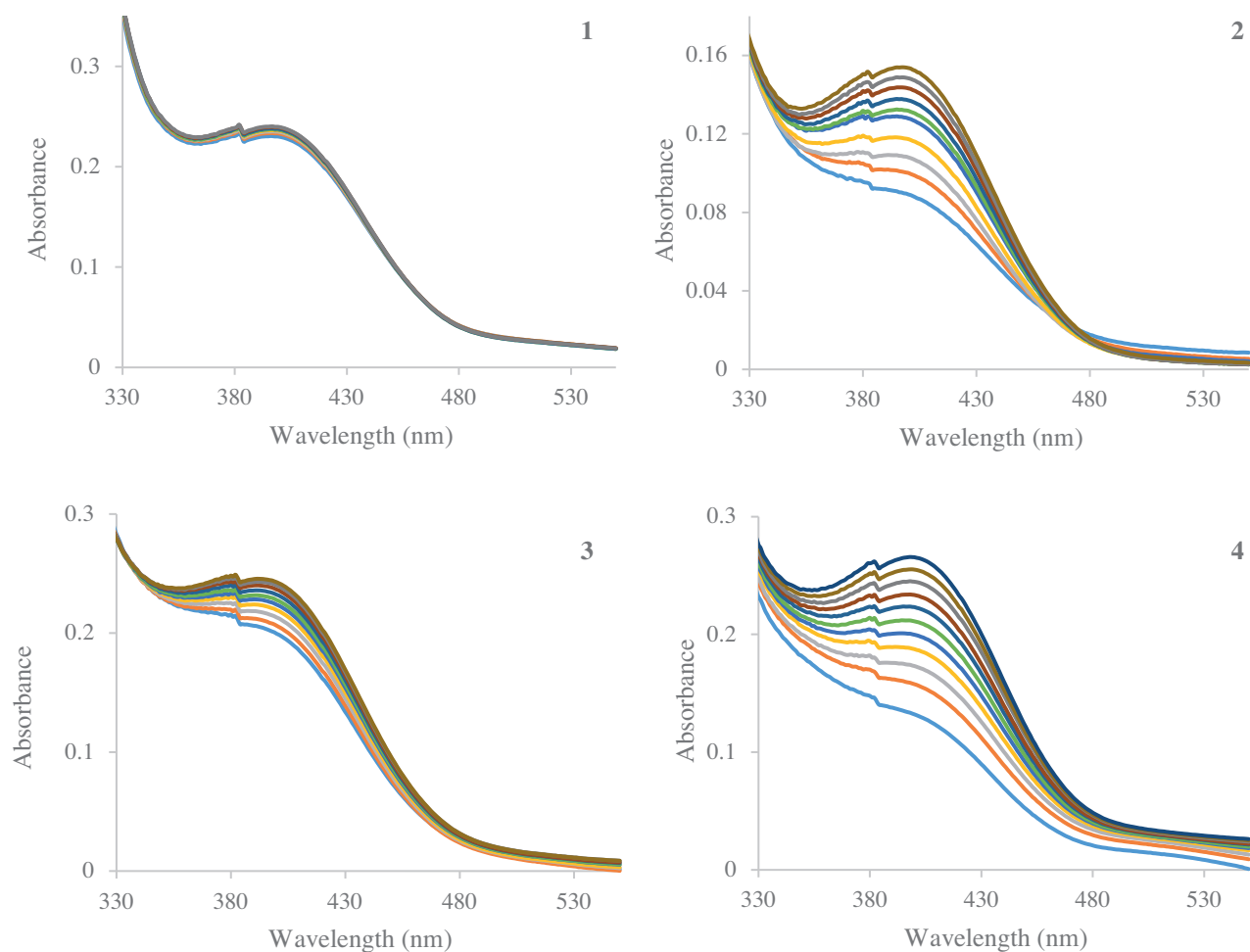


Figure 2. Increase in the quinone band at ~ 399 nm after addition of 100 equivalents of 3,5-DTBC to solutions of 1–4 in DMF at 25 °C. The spectra were recorded at an interval of 5 min.

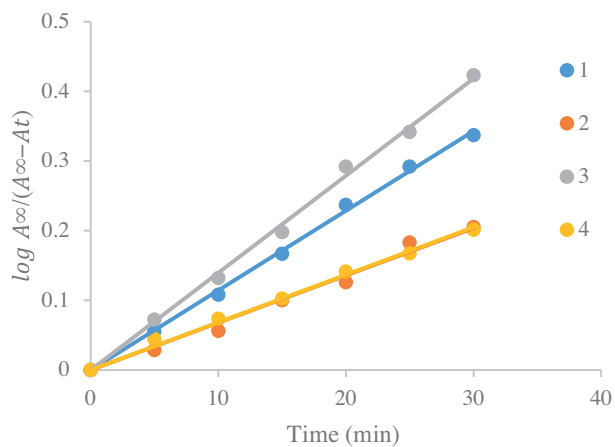


Figure 3. Catecholase activity of complexes 1–4.

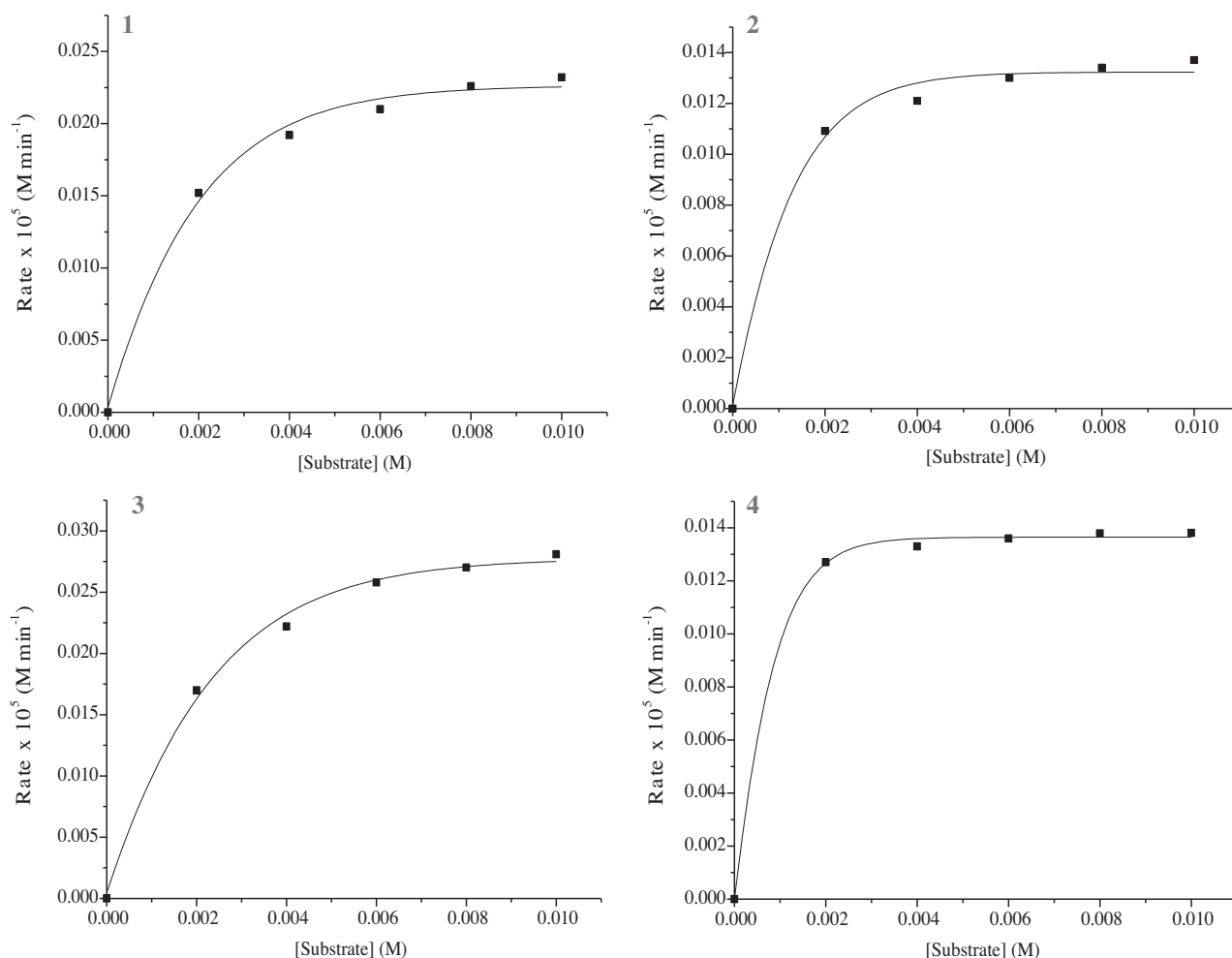


Figure 4. Plot of the initial rates versus substrate concentration for the oxidation of 3,5-DTBC catalysed by 1–4.

to the Cu(I) centre, producing Cu(II)-coordinated superoxo species, which rapidly gains electrons from the coordinated semiquinone radical to convert it to coordinated hydroperoxide. The semiquinone is thus converted to quinone, which dissociates from the metal coordination sphere along with H_2O_2 and the active Cu(II)-catalyst is regenerated. Similar mechanisms of DTBC oxidation by some mononuclear complexes, which passes through the semiquinone intermediate, have been proposed by some earlier workers.^{26–28}

3. Experimental

3.1. Materials and physical measurements

Piperazine, p-acetamidophenol, formaldehyde solution, potassium thiocyanate, DMSO- d_6 , and 3, 5-di-tert-butylcatechol were purchased from Sigma Aldrich and used as such. Methanol, isopropanol, and chloroform were purchased from Sigma Aldrich. All chemicals and solvents were of analytical grade and used as received without purification. The metal salts used were in hydrated form, i.e. $\text{CuCl}_2 \cdot 2\text{H}_2\text{O}$ (copper(II) chloride dihydrate) and $\text{FeCl}_3 \cdot 6\text{H}_2\text{O}$ (iron(III) chloride hexahydrate).

Elemental analysis (C, H, N, and S) was carried out using an Elementar Analysensysteme VarioMICRO

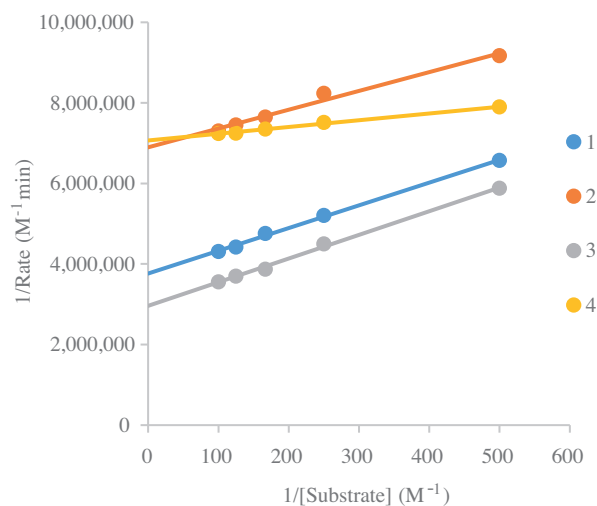
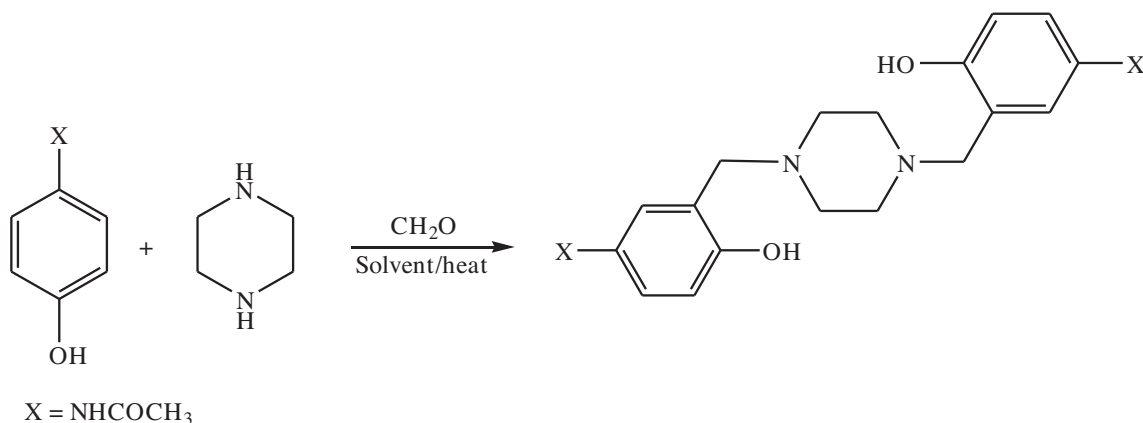


Figure 5. Lineweaver–Burk plots for the metal complexes **1–4**.

V1.62 GmbH analysis System. NMR spectra (^1H and ^{13}C NMR) were acquired in $\text{DMSO-}d_6$ using a Bruker AMX 300 MHz spectrometer with tetramethylsilane (TMS) as an internal standard for ^1H . Electronic spectra were recorded for the solutions of the ligand and metal complexes in DMF and DMSO on a PerkinElmer UV-Vis spectrophotometer model Lambda 25. Attenuated total reflection Fourier transform infrared (ATR-FTIR) spectra for all the samples were recorded on a PerkinElmer Spectrum400 spectrophotometer in the range $4000\text{--}650\text{ cm}^{-1}$. Molar conductivities were measured in DMSO using a 10^{-3} M solution of the compounds on an AZ 86555 conductivity meter. The melting points were determined on a Gallenhamp melting point apparatus.

3.2. Synthesis of the Mannich ligand (H_2L)

The synthesis of the ligand [1,4-di-(5-acetamido-2-hydroxybenzyl)piperazine] was carried out according to the Scheme below.



Scheme. Synthesis of Mannich base (H_2L).

The Mannich base herein studied has been encountered in the series of compounds reported by Agrawal and Sharma with the spectroscopic data unreported.²⁹ The method by Sriram et al.³⁰ was adopted in the

synthesis of this ligand with a slight modification made. 4-Acetamidophenol (20 mmol, 3.023 g), formaldehyde solution (37%) (1.51 mL, 20 mmol), and piperazine (10 mmol, 0.8614 g) were suspended in 10 mL of isopropyl alcohol and heated in a steam bath for 12 h. The progress of the reaction was monitored with TLC and cooling the reaction mixture upon completion led to the formation of a crystalline solid. This was collected and washed with isopropyl alcohol. Recrystallization was carried out in a chloroform:ethanol mixture to give a white crystalline solid. White solid, Yield 74%, mp: 241 °C, Anal. Cald (%) for $C_{22}H_{28}N_4O_4$, C, 64.06; H, 6.84; N, 13.58. Found: C, 63.59; H, 7.16; N, 13.20%. 1H NMR (DMSO- d_6): 2.38 (s, 6H, CH_3CONH-), 2.90 (s, 8H, $(CH_2)_2N-$), 3.97 (s, 4H, Ar- CH_2), 7.06–7.71 (m, 6H, Ar-H). ^{13}C NMR ($CDCl_3$): 23.7, 52.0, 58.3, 115.3–168.2. IR bands (ATR-FTIR, cm^{-1}): 3250, 1297, 1141. Electronic spectra (DMF, cm^{-1}); 37,037, 33,670 (DMSO, cm^{-1}) 33,445.

3.3. Synthesis of metal complexes

All the four metal complexes (1–4) were prepared by a general procedure. To the solution of the ligand (5 mmol) in 5 mL of warm chloroform was added an equimolar 5 mmol methanolic solution of the hydrated metal chloride salt. The preparation of the thiocyanate metal complex involved the addition of an equal mole of potassium thiocyanate dissolved in methanol. Also the synthesis of the Fe(III) complexes involved the addition of a few drops of triethylamine as deprotonating agent. The resulting mixture was stirred at room temperature for 6 h, the precipitate was filtered off, and it was washed twice with a 1:1 methanol:chloroform mixture.

3.3a [$Cu_2LCl_2 \cdot 2H_2O$] (1): Yield 49%: mp: 161 °C. Anal. Cald (%) for $Cu_2C_{22}H_{26}N_4O_4Cl_2 \cdot 2H_2O$: C, 40.87; H, 4.37; N, 8.67. Found: C, 40.81, H, 4.59; N, 8.79. $\Lambda_M = 31.65 \Omega^{-1} cm^2 mol^{-1}$. IR bands (ATR-FTIR, cm^{-1}): 3274, 1259, 1119. Electronic spectra (DMF, cm^{-1}); 36,765, 33,113, 21,459 (DMSO, cm^{-1}); 32,154, 28,653, 20,921, 11,682.

3.3b [$Cu_2H_2L(NCS)_2 \cdot 2H_2O$] $Cl_2 \cdot H_2O$ (2): Yield 61%: mp: >250 °C. Anal. Cald (%) for $Cu_2C_{24}H_{28}N_6O_4S_2Cl_2 \cdot 4H_2O$: C, 36.09; H, 4.52; N, 10.52; S, 8.01. Found: C, 36.32; H, 4.60; N, 10.54; S, 8.38. $\Lambda_M = 60.65 \Omega^{-1} cm^2 mol^{-1}$. IR bands (ATR-FTIR, cm^{-1}): 3290, 2106(sp), 1260, 1070, 749. Electronic spectra (DMF, cm^{-1}); 37,175, 30,211, 16,103 (DMSO, cm^{-1}) 32,680, 22,779, 14,970.

3.3c [FeH_2LCl_3] $3H_2O$ (3): Yield 42%: mp: 191 °C. Anal. Cald (%) for $FeC_{22}H_{28}N_4O_4Cl_3 \cdot 3H_2O$: C, 42.01; H, 5.45; N, 8.90. Found: C, 41.61, H, 5.69; N, 8.79 $\Lambda_M = 37.24 \Omega^{-1} cm^2 mol^{-1}$. IR bands (ATR-FTIR, cm^{-1}): 3299, 1255, 1116. Electronic spectra (DMF, cm^{-1}); 32,787, 27,397, 18,797 (DMSO, cm^{-1}) 35,461, 28,736.

3.3d [$Fe_2H_2L(NCS)_2 \cdot 2H_2O \cdot \frac{1}{2}CHCl_3$] $Cl_4 \cdot 2H_2O$ (4): Yield 46%: mp: 181 °C. Anal. Cald (%) for $Fe_2C_{24}H_{28}N_6O_4S_2Cl_4 \cdot 4H_2O \cdot \frac{1}{2}CHCl_3$: C, 32.22; H, 4.02; N, 9.13; S, 7.02. Found: C, 31.98, H, 3.73; N, 9.23; S, 7.14 $\Lambda_M = 129.83 \Omega^{-1} cm^2 mol^{-1}$. IR bands (ATR-FTIR, cm^{-1}): 3253 (br), 2035 (br), 1260, 1118, 798. Electronic spectra (DMF, cm^{-1}); 32,051, 27,322, 25,381, 21,645 (DMSO, cm^{-1}) 32,051, 28,329, 21,368.

3.4. Catalytic oxidation of 3,5-DTBC

Evaluation of the catecholase activity of the complexes (1–4) was carried out by treating 10^{-4} M solution of the complexes in DMF with 100 equiv. of 3,5-di-tert-butylcatechol (3,5-DTBC) under aerobic conditions at room temperature. Spectral scans were recorded at a regular time interval of 5 min in the wavelength range 330–550 nm.

Amongst the various catechols used in catechol oxidase model studies, 3,5-DTBC is the most widely used because its low redox potential for the quinone/catechol couple leads to easy oxidation to a highly stable corresponding quinone (3,5-DTBQ).^{31,32}

Kinetic experiments (using the method of initial rates) were performed while keeping the concentration of metal complexes constant at 1×10^{-4} M and varying the concentration of the substrate (1×10^{-3} M to 1×10^{-2} M) in DMF using a UV-Vis spectrophotometer. The formation of 3,5-DTBQ was monitored over time at a wavelength of 399 nm with each experiment carried out in duplicate. The kinetic experiment was followed by the detection of H_2O_2 to provide information on the mechanism of catalytic behaviour according to a method previously reported in the literature.^{33,34}

4. Conclusions

Summarily, we have succeeded in synthesising a new Mannich base of 4-acetamidophenol and compared the catecholase activity of its Cu(II) and Fe(III) complexes. All the metal complexes show moderately high turnover rates. The presence of thiocyanate within the metal complex leads to a reduction in catecholase activity. We have also shown that geometry plays a huge role in catalytic abilities of metal complexes like in the case of **1**. The identification of H_2O_2 and isolation of benzoquinone reveal the presence of Cu(I) species during the oxidative process.

Acknowledgement

The authors wish to thank Rhodes University, South Africa, for supporting this research.

References

- Solomon, E. I.; Sarangi, R.; Woertink, J. S.; Augustine, A. J.; Yoon, J.; Ghosh, S. *Acc. Chem. Res.* **2007**, *40*, 581–591.
- Simandi, L. I. *Advances in Catalytic Activation of Dioxygen by Metal Complexes*; Dordrecht, Netherlands: Academic Publishers, 1992.
- Kovaleva, E. G.; Neibergall, M. B.; Chakrabarty, S.; Lipscomb, J. D. *Acc. Chem. Res.* **2007**, *40*, 475–483.
- Itoh, S.; Fukuzumi, S. *Acc. Chem. Res.* **2007**, *40*, 592–600.
- Pierpoint, W. S. *Biochem. J.* **1969**, *112*, 609–616.
- Ohlendorf, D. H.; Lipscomb, J. D.; Weber, P. C. *Nature* **1988**, *336*, 403–405.
- Ohlendorf, D. H.; Orville, A. M.; Lipscomb, J. D. *J. Mol. Biol.* **1994**, *244*, 586–608.
- Rogic, M. M.; Swerdloff, M. D.; Demmin, T. R. In *Copper Coordination Chemistry: Biochemical and Inorganic Perspectives*, Karlin, K. D.; Zubieta, J., Eds. Adenine: Guilderland, NY, USA, 1983.
- Comba, P.; Wadepohl, H.; Wunderlich, S. *Eur. J. Inorg. Chem.* **2011**, 5242–5249.
- Anbu, S.; Kandaswamy, M. *Polyhedron* **2011**, *30*, 123–131.
- Ali, I.; Wani, W. A.; Saleem, K. *Synth. React. Inorg. Met.-Org. Chem.* **2013**, *43*, 1162–1170.
- Brycki, B.; Maciejewska, H.; Brzezinski, B.; Zundel, G. *J. Mol. Struct.* **1991**, *246*, 61–71.
- Raj, S. S.; Ponnuswamy, M. N.; Shanmugam, G.; Kandaswamy, M. *J. Chem. Cryst.* **1994**, *24*, 83–87.
- Yilmaz, V. T.; Guney, S.; Harrison, W. T. A. *Z. Naturforsch.* **2005**, *60b*, 403–407.
- You, Z. L.; Zhang, L.; Shi, D. H.; Wang, X. L.; Li, X. F.; Ma, Y. P. *Inorg. Chem. Commun.* **2010**, *13*, 996–998.

16. Bhat, I.; Tabassum, S. *Spect. Acta A* **2009**, *72*, 1026–1033.
17. Kabesova, M.; Gazo, J. *Chem. Zvesti* **1980**, *34*, 800–841.
18. Al-Jeboori, M. J.; Abdul-Ghani, A. J.; Al-Karawi, A. J. *Transition Met. Chem.* **2008**, *33*, 925–930.
19. Manonmani, J.; Kandaswamy, M.; Narayanan, V.; Thirumurugan, R.; Raj, S. S.; Shanmugam, G.; Ponnuswamy, M. N.; Fun, H. K. *Polyhedron* **2001**, *20*, 3039–3048.
20. Garg, S. B.; Kurup, M. R. P.; Jain, S. K. *Tran. Met. Chem.* **1988**, *13*, 247–249.
21. Dey, D.; Das, S.; Yadav, H. R.; Ranjani, A.; Gyathri, L.; Roy, S.; Guin, P. S.; Dhanasekaran, D.; Choudhury, A. R.; Akbarsh, M. A.; et al *Polyhedron* **2016**, *106*, 106–114.
22. Ramadan, A. E. M.; Shaban, S. Y.; Ibrahim, M. M. *J. Coord. Chem.* **2011**, *64*, 3376–3392.
23. Panja, A. *Polyhedron* **2014**, *80*, 81–89.
24. De, A.; Dey, D.; Yadav, H. R.; Rane, M. M.; Kadam, R. M.; Choudhury, A. R.; Biswas, B. *J. Chem. Sci.* **2016**, *128*, 1775–1782.
25. Reim, J.; Krebs, B. *J. Chem. Soc. Dalton* **1997**, 3793–3804.
26. Reim, J.; Werner, R.; Hasse, W.; Krebs, B. *Chem. Eur. J.* **1998**, *4*, 289–298.
27. Gajewska, M. J.; Ching, W. M.; Wen, Y. S.; Hung, C. H. *Dalton T.* **2014**, *43*, 14726–14736.
28. Shyamal, M.; Mandal, T. K.; Panja, A.; Saha, A. *RSC Adv.* **2014**, *4*, 53520–53530.
29. Agrawal, V. K.; Sharma, S. *Ind. J. Chem. Section B*, **1987**, *26b*, 550–555.
30. Sriram, D.; Devakaram, R. V.; Dinakaran, M.; Yogeeswari, P. *Med. Chem. Res.* **2010**, *19*, 524–532.
31. Biswas, A.; Das, L. K.; Drew, M. G. B.; Aromi, G.; Gamez, P.; Ghosh, A. *Inorg. Chem.* **2012**, *51*, 7993–8001.
32. Mukherjee, J.; Mukherjee, R. *Inorg. Chim. Acta* **2002**, *337*, 429–438.
33. Vogel, A. I. *Textbook of Quantitative Inorganic Analysis*; 3rd edn, Longmans, Green and Co. Ltd: London, UK, 1961.
34. Monzani, E.; Quinti, L.; Perotti, A.; Casella, L.; Gullotti, M.; Randaccio, L.; Geremia, S.; Nardin, G.; Faleschini, P.; Tabbi, G. *Inorg. Chem.* **1998**, *37*, 553–562.